Toxicology and Applied Pharmacology 274 (2014) 393–401

Contents lists available at ScienceDirect

Toxicology and Applied Pharmacology

journal homepage: www.elsevier.com/locate/ytaap

Functional characterization of cytochromes P450 2B from the desert woodrat *Neotoma lepida*

P. Ross Wilderman [a,*], Hyun-Hee Jang [a], Jael R. Malenke [b], Mariam Salib [a,1], Elisabeth Angermeier [a,2], Sonia Lamime [a,3], M. Denise Dearing [b], James R. Halpert [a]

[a] Skaggs School of Pharmacy and Pharmaceutical Sciences, University of California, San Diego, La Jolla, CA, USA
[b] Department of Biology, University of Utah, Salt Lake City, UT, USA

ARTICLE INFO

Article history:
Received 23 October 2013
Revised 9 December 2013
Accepted 10 December 2013
Available online 19 December 2013

Keywords:
Biotransformation
Woodrats
Cytochrome P450
Juniper
Detoxification

ABSTRACT

Mammalian detoxification processes have been the focus of intense research, but little is known about how wild herbivores process plant secondary compounds, many of which have medicinal value or are drugs. cDNA sequences that code for three enzymes of the cytochrome P450 (CYP) 2B subfamily, here termed 2B35, 2B36, and 2B37 have been recently identified from a wild rodent, the desert woodrat (Malenke et al., 2012). Two variant clones of each enzyme were engineered to increase protein solubility and to facilitate purification, as reported for CYP2B enzymes from multiple species. When expressed in *Escherichia coli* each of the woodrat proteins gave the characteristic maximum at 450 nm in a reduced carbon monoxide difference spectrum but generally expressed at lower levels than rat CYP2B1. Two enzymes, 2B36 and 2B37, showed dealkylation activity with the model substrates 7-ethoxy-4-(trifluoromethyl)coumarin and 7-benzyloxyresorufin, whereas 2B35 was inactive. Binding of the monoterpene (+)-α-pinene produced a Type I shift in the absorbance spectrum of each enzyme. Mutation of 2B37 at residues 114, 262, or 480, key residues governing ligand interactions with other CYP2B enzymes, did not significantly change expression levels or produce the expected functional changes. In summary, two catalytic and one ligand-binding assay are sufficient to distinguish among CYP2B35, 2B36, and 2B37. Differences in functional profiles between 2B36 and 2B37 are partially explained by changes in substrate recognition site residue 114, but not 480. The results advance our understanding of the mechanisms of detoxification in wild mammalian herbivores and highlight the complexity of this system.

Introduction

Cytochrome P450 (CYP)-dependent monooxygenases are a crucial superfamily of enzymes involved in the metabolism of numerous endogenous and xenobiotic compounds, including many pharmaceuticals (Johnson and Stout, 2013). CYPs are found in all multi-cellular organisms. These enzymes carry out Phase I metabolism of hydrophobic substrates through a variety of mechanisms, thereby rendering the compounds more hydrophilic to facilitate excretion or subsequent conjugation (Al Omari and Murry, 2007; Guengerich and Isin, 2008). In mammals, particularly herbivorous ones, CYPs likely arose as a protective response to the rapid evolution of chemical diversity in plants (Gonzalez, 1988; Stamp, 2003; Weng et al., 2012). Along with the central role in drug clearance, activation of prodrugs via CYPs also contributes to the importance of these enzymes in the pharmaceutical and healthcare industries (Guengerich, 2001; Ingelman-Sundberg, 2004).

CYPs accept a broad array of compounds as substrates, utilizing a highly conserved protein fold consisting of a largely α-helical domain and a domain dominated by β-sheets (Anzenbacher et al., 2008; Poulos, 2005a). The broad substrate specificity is due in part to the high degree of flexibility previously observed in these enzymes (Gay et al., 2010; Otyepka et al., 2012; Poulos, 2005b; Wilderman and Halpert, 2012). In addition to exhibiting considerable conformational plasticity, members of the CYP2B subfamily also show relatively low conservation of catalytic activity across mammalian species, making a good system for exploration of structure–function relationships within and across mammalian species (Zhao and Halpert, 2007). Studies of

Abbreviations: CYP, cytochrome P450-dependent monooxygenases; ITC, isothermal titration calorimetry; DXMS, hydrogen–deuterium exchange coupled to mass spectrometry; 7-EFC, 7-ethoxy-4-(trifluoromethyl)coumarin; 7-BR, 7-benzyloxyresorufin; 2BXdH, an *N*-terminally truncated and modified 2B enzyme with a *C*-terminal tetra-His tag to facilitate purification; BME, 2-mercaptoethanol; PMSF, phenylmethanesulfonyl fluoride; CHAPS, 3-[(3-cholamidopropyl)dimethylammonio]-1-propanesulfonate; EDTA, ethylenediaminetetraacetic acid; DTT, dithiotheitol; PSC, plant secondary compound or plant specialized compound; HS_{P450}, high spin P450.

* Corresponding author at: Skaggs School of Pharmacy and Pharmaceutical Sciences, University of California, San Diego, 9500 Gilman Dr., MC 0703, La Jolla, CA 92093-0703, USA.
E-mail address: pwilderman@ucsd.edu (P.R. Wilderman).
[1] Present Address: Department of Molecular and Experimental Medicine, The Scripps Research Institute, La Jolla, California, USA.
[2] Present Address: Institute of Pharmacology and Toxicology, Technical University Munich, Munich, Germany.
[3] Present Address: Institut Superieur des Biosciences de Paris, Universite UPEC—Faculte de Medecine, Paris, France.

0041-008X/$ – see front matter © 2013 Elsevier Inc. All rights reserved.
http://dx.doi.org/10.1016/j.taap.2013.12.005

CYP2B enzymes have yielded a substantial body of biochemical and biophysical information relating to protein–ligand and protein–protein interactions and the catalytic mechanisms of microsomal monooxygenases. Studies utilizing isothermal titration calorimetry (ITC) and hydrogen/deuterium exchange coupled to mass spectrometry (DXMS) reinforced our understanding of the ability of the rabbit 2B4 to bind to a wide range of ligands in solution (Muralidhara et al., 2006; Wilderman and Halpert, 2012).

Despite the wealth of information concerning detoxification enzymes in model systems, interactions between plants and herbivores are more complex, and knowledge of the contributions of CYP enzymes to the biotransformation of plant secondary compounds in wild mammalian species is generally lacking (Al Omari and Murry, 2007; Dearing et al., 2005). Plant secondary compounds are metabolites that are not essential for the life of a plant, but may play a role in defense and are usually byproducts of primary metabolism. Molecular characterization of enzymes from wild populations is necessary for elucidating biotransformation mechanisms in wild herbivores. Unfortunately, genetic information on CYPs is available for only a small number of such species. Recent studies document involvement of CYPs in detoxification processes in koalas (*Phascolarctos cinereus*) and in several species of woodrats (*Neotoma lepida*) (El-Merhibi et al., 2008; Haley et al., 2007a,b, 2008; Magnanou et al., 2009; Skopec et al., 2007). Furthermore, members of the 3A subfamily of CYPs were recently characterized from koala and the Eastern gray kangaroo (*Macropus giganteus*) (El-Merhibi et al., 2011, 2012) and the 4A subfamily in the koala and common bush tail possum (*Trichosurus vulpecula*) (Ngo et al., 2003, 2006).

To advance knowledge of CYP enzymes in herbivores, we characterized members of the CYP2B subfamily of enzymes from desert woodrats (*N. lepida*). This species was selected because it has a wide distribution across the southwestern USA, and individuals ingest a wide variety of secondary compounds such as terpenes and phenols depending on the availability of plant species in the habitat (Mangione et al., 2000). Sequence analysis of a large number of cDNA sequences from individual animals produced four major CYP2B clades (A, F, G, and H) that have different numbers of unique clones depending on home habitat and laboratory diet (Malenke et al., 2012). To initiate our investigation of the molecular mechanisms of plant–animal interactions mediated by detoxification enzymes we modified cDNA clones from clades A, F, and H to produce engineered proteins with a truncated and modified *N*-terminal region and a *C*-terminal tetra-His tag. These proteins were expressed, and the enzymes were characterized utilizing 7-ethoxy-4-trifluoromethyl coumarin (7-EFC) and 7-benzyloxyresorufin (7-BR) as substrates and the monoterpene (+)-α-pinene as a ligand probe. Results from these assays were compared with those from rat 2B1. The effects of mutations at residues corresponding to known polymorphisms in the human 2B6 (262) or known to alter substrate specificity and/or product profile in other 2B enzymes (114 and 480) were also explored. Two catalytic assays and one binding assay yielded unique results for each of the woodrat 2B enzymes, and subset of residues previously identified as governing substrate specificity, product production, or ligand binding affinity showed smaller changes in catalytic efficiency than expected. These findings highlight the overall complexity of the detoxification mechanisms utilized by wild mammalian herbivore.

Methods

Materials. All reagents were of the highest grade commercially available and were used without further purification. Macroprep CM-Sepharose cation exchange resin was from Bio-Rad Laboratories (Hercules, CA). *TOPP3* cells were from Stratagene (La Jolla, CA). Primers were synthesized by Integrated DNA Technologies (Coralville, IA).

Clone selection. The clones chosen for functional characterization were part of a large dataset of CYP2B cDNAs compiled from individuals of two desert woodrat populations from either the Mojave Desert or Great Basin (Malenke et al., 2012). Prior to genetic sampling, individuals were fed a diet including plant secondary compounds from either juniper (*Juniperus osteosperma*) or creosote bush (*Larrea tridentata*). These two plants are representative of the wild diets of the past and present diets of woodrats in the Mojave Desert, respectively. For additional information regarding the diets and feeding trial, see Malenke et al. (2012).

Woodrat 2B cDNA identification was performed as previously described (Malenke et al., 2012). Briefly, primers were designed from a search of Genbank for deposited 2B genes. Full open reading frames were acquired using rapid amplification of cDNA ends (First Choice RLM-RACE kit, Life Technologies, Carlsbad, CA) following the manufacturers' protocol. Sequences were compared to deposited sequences from rat (*Rattus norvegicus*, CYP2B1 and CYP2B3), mouse (*Mus musculus*, CYP2B9 and CYP2B10), and human (*Homo sapiens*, CYP2B6). Variants were categorized into clades using phylogenetic analysis, and the different clades displayed variation at known substrate recognition site (SRS) residues (Malenke et al., 2012; Wilderman and Halpert, 2012). Two clones were chosen from each of three clades: A—2B35v1/2, F—2B36v1/2, and H—2B37v1/2 (GenBank: JN105889—2B35v1, JN105900—2B35v2, JN105951—2B36v1, JN105955—2B36v2, JN105945—2B37v1 and JN105939—2B37v2). It is unknown whether the variant proteins in each clade represent unique alleles or different loci in the CYP2B subfamily. Full length clones were in either the pCR®2.1-TOPO® plasmid (2B35v2, 2B36v1/2, and 2B37v1) or the pCR™4-TOPO® plasmid (2B35v1 and 2B37v2) from Life Technologies (Grand Island, NY).

Sequence alignment, protein engineering, and site-directed mutagenesis. Sequence alignments and identity calculations were performed with Geneious v. 6.1.3 from Biomatters Ltd. (Auckland, New Zealand), using standard parameters. 2B1 was the reference sequence in all cases. Engineering efforts were performed as previously described (Scott et al., 2001). Sequences for all primers used in protein engineering efforts are contained in Table S1.

For 2B35v1, both variants of 2B36, and 2B37v1, the engineered gene was created using two PCR reactions. For 2B35v1 and 2B36v2, the first reaction contained the T7 primer as a forward primer and a reverse primer containing the native C-terminal end of the enzyme, four His codons, the stop codon, and an *Eco*RV recognition site (NSpdH R2—2B35v1; NSpdH R—2B36v2). For 2B36v1 and 2B37v1, the first reaction contained the M13 reverse primer as a forward primer and the NSpdH R primer as the reverse primer. Prior to engineering 2B37v1, an internal *Nco*I recognition sequence was removed by introduction of a silent mutation (*Nco*I site removal primers in Table S1). Site directed mutagenesis was performed using primers for the desired sequence modifications and an appropriate PCR protocol. For these constructs, the second reaction contained a forward primer containing the 5′-truncation and modifications along with an *Nco*I recognition site (NSpdH F) the reverse primers used in the first reaction. A single PCR reaction was used to engineer 2B35v2 and 2B37v2 using NSpdH F as the forward primer and NSpdH R2 (2B35v2) or NSpdH R (2B37v2) as the reverse primer. The product of these reactions was purified using Macherey-Nagel NucleoSpin® Gel and PCR Clean-Up from Clontech (Mountain View, CA). Following clean up the PCR product for both variants of 2B35 and 2B37 was digested with *Nco*I and *Eco*RV and ligated into a similarly cut pKK2B4dH plasmid. Successful insertion of the engineered 2B36 variants into this vector required use of the In-Fusion® HD Cloning Kit from Clontech using the standard protocol from the kit. Construct sequences were verified at Retrogen, Inc. (San Diego, CA).

For site-directed mutagenesis, single mutants were created using as a template the plasmid that containing the protein of interest, along with appropriate forward and reverse primers (Table S2). Mutants were generated by PCR using Phusion High-Fidelity DNA Polymerase and a standard site-directed mutagenesis protocol. Constructs were sequenced at Retrogen, Inc.

Protein expression and purification. CYP2B enzymes were expressed in *TOPP3* cells as previously described (Scott et al., 2001) and purified by the protocol used by Shah et al. (2012). The pellet was resuspended in 10% of the original culture volume in buffer containing 20 mM potassium phosphate (pH 7.4 at 4 °C), 20% (v/v) glycerol, 10 mM 2-mercaptoethanol (BME), and 0.5 mM phenylmethanesulfonyl fluoride (PMSF). The resuspended cells were further treated with lysozyme (0.3 mg/mL) and stirred for 30 min, followed by centrifugation for 30 min at 7000 rpm in a JA-14 rotor in a Beckman Coulter Avanti J-26 XPI Centrifuge. After decanting the supernatant, spheroplasts were re-suspended in 5% of the original culture volume in buffer containing 500 mM potassium phosphate (pH 7.4 at 4 °C), 20% (v/v) glycerol, 10 mM BME, and 0.5 mM PMSF and were sonicated for 3 × 45 s on ice. 3-[(3-Cholamidopropyl)dimethylammonio]-1-propanesulfonate (CHAPS) was added to the sample at a final concentration of 0.8%, and this was allowed to stir for 30 min at 4 °C prior to ultracentrifugation for 45 min at 41,000 rpm using a fixed-angle Ti 50.2 rotor in a Beckman Coulter Optima L-80 XP Ultracentrifuge. The CYP concentration was measured using the reduced CO difference spectra from the resulting supernatant (Omura and Sato, 1964; Omura et al., 1965).

The supernatant was applied to a Ni^{2+}-NTA column. The column was washed with buffer containing 100 mM potassium phosphate (pH 7.4 at 4 °C), 100 mM NaCl, 20% (v/v) glycerol, 10 mM BME, 0.5 mM PMSF, 0.5% CHAPS and 5 mM histidine, and the protein was eluted using buffer containing 10 mM potassium phosphate (pH 7.4 at 4 °C), 100 mM NaCl, 20% (v/v) glycerol, 10 mM BME, 0.5 mM PMSF, 0.5% CHAPS, and 50 mM histidine. Protein fractions containing protein of the highest quality as measured by the A_{417}/A_{280} ratios were pooled, and the CYP concentration in the eluted fractions was measured using the reduced CO difference spectra. The CYP containing fractions were pooled and loaded onto a Macroprep CM-Sepharose column. The cation exchange column was washed using low salt buffer containing 5 mM potassium phosphate (pH 7.4 at 4 °C), 20% (v/v) glycerol, 1 mM EDTA, and 0.2 mM DTT. The protein was eluted with high salt buffer containing 50 mM potassium phosphate (pH 7.4 at 4 °C), 500 mM NaCl, 20% (v/v) glycerol, 1 mM EDTA and 0.2 mM DTT. Protein fractions containing protein of the highest quality as measured by the A_{417}/A_{280} ratios were pooled, and the CYP fractions were pooled and the concentration was measured using the reduced CO-difference spectra.

Enzymatic assays. The standard NADPH-dependent assay for 7-EFC or 7-BR *O*-dealkylation by 2B enzymes was carried out as described previously (He et al., 1995; Kumar et al., 2005). The reconstituted system contained the following recombinant proteins at a molar ratio of 1:4:2 cytochrome P450, rat NADPH-cytochrome P450 reductase (Harlow and Halpert, 1997), and rat cytochrome b_5 (Holmans et al., 1994) as previously optimized (Scott et al., 2001).

Reactions for using 7-EFC were carried out using the reconstituted system in a 100 μl final volume and substrate at varying concentrations (0–150 μM). Assays were performed in buffer containing 50 mM HEPES (pH 7.4) and 15 mM $MgCl_2$, initiated by addition of NADPH to a final concentration of 1 mM and incubated for 10 min at 37 °C. Ice cold acetonitrile was added to quench the reaction. An aliquot of the reaction was then transferred to a glass tube containing 0.1 M Tris (pH 9.0), and fluorescence was determined with excitation at 410 nm and emission at 510 nm for 7-HFC using a Cary Eclipse Fluorimeter (Agilent, Santa Clara, CA).

Reactions for the 7-BR assay were carried out using the reconstituted system in a 500 μl final volume and substrate at varying concentrations (0–10 μM). Assays were performed in buffer containing 50 mM HEPES (pH 7.4) and 15 mM $MgCl_2$, initiated by addition of NADPH to a final concentration of 1 mM and incubated for 10 min at 37 °C. Methanol (2 mL) was added to quench the reaction. Fluorescence was determined with excitation at 550 nm and emission at 580 nm for resorufin using a Hitachi F2000 fluorescence spectrophotometer (Tokyo, Japan).

In both assays calibration was performed at the end of each day by measuring the intensity of fluorescence in a series of four to five samples of the same reaction mixture containing HFC or resorufin at concentrations from 0 to 2 μM. Steady state kinetic parameters were determined by regression analysis using SPECTRALAB (Davydov et al., 1995). Values of catalytic constants were determined using the Michaelis–Menten equation. Kinetic experiments included wild-type and mutant enzymes for more accurate comparison of the data.

Spectral binding titrations. The absorbance spectra were measured with an MC2000-2 multi-channel CCD rapid scanning spectrometer (Ocean Optics, Dunedin, FL, USA) equipped with one absorbance and one fluorescence channel, a pulsed Xe-lamp PX-2 light source, and a custom thermostated cell chamber with a magnetic stirrer. A semi-micro quartz cell with a stirring compartment (10 × 4 mm light path) from Hellma GmbH (Müllheim, Germany) was used in the titration experiments. All titration experiments were carried out at 25 °C with continuous stirring in buffer containing 100 mM HEPES (pH 7.4 at 4 °C), 20% glycerol, and 100 mM KCl. A baseline was recorded between 340 and 700 nm using this buffer. A spectrum was recorded after the addition of protein to the buffer. Spectra were recorded after the addition of aliquots of ligand to the sample cuvette. The spectral dissociation constants (K_S) were obtained by fitting the data to the equation for ligand binding for high affinity ligands $2\Delta A = (\Delta A_{max} / [E_0])((K_S + [L_0] + [E_0]) - (K_S + [L_0] + [E_0])^2 - 4[E_0][L_0])^{1/2})$ where ΔA_{max} is the maximum change in the percent high-spin P450 (HS_{P450}), E_0 is total enzyme concentration, and L_0 is total ligand concentration when data are normalized to total CYP concentration using SPECTRALAB (Davydov et al., 1995). The mean differences in the change in % HS_{P450} values between mutant and wild-type enzymes were compared using an independent sample *t*-test (Microsoft Excel 2011, Redmond, WA, USA).

Figures. All protein model figures were generated using PyMOL (DeLano, 2009). All chemical structures were created using MarvinSketch v. 5.2.6, 2009, ChemAxon (http://www.chemaxon.com). Figures depicting spectral data were created using Igor Pro 6.2 (Wavemetrics Inc., Lake Oswego, OR, USA).

Results

Sequence alignment and protein engineering

In the interest of expanding the understanding of structure–function relationships of CYP2B enzymes, six previously isolated cDNAs from desert woodrats (*N. lepida*) were engineered in the same manner as 2B1 (Malenke et al., 2012; Scott et al., 2001). Extensive prior results have documented that the *N*-terminal truncation and modification and the addition of a tetra-His tag to CYP2B enzymes increase protein expression levels, facilitate solubilization using high salt conditions, and result in high purity after chromatography with minimal impact on function. Fig. 1A shows the *N*-terminal and *C*-terminal regions of the engineered 2B1dH and full-length 2B35v1, 2B35v2, 2B36v1, 2B36v2, 2B37v1, and 2B37v2. The cDNA sequences of the woodrat enzymes were among those reported by Dearing and coworkers (Malenke et al., 2012).

An alignment of the engineered 2B1dH and the full-length enzymes from woodrat is in Supplementary Fig. S1. Using the previous notation 2B35v1/2 are from Clade A, 2B36v1/2 are from Clade F, and 2B37v1/2 are from Clade H. Variants of each enzyme display ≥98% identity to each other across 491 amino acids. 2B35, 2B36, and 2B37 show roughly 90–95% amino acid identity between enzymes when compared pairwise. The Clade A and Clade F variant enzymes contain two amino acid differences apiece (2B35v1/2—G2E and F408L; 2B36v1/2—L8P and Q45R); in both pairs of enzymes only one of the differences is found in the engineered enzyme (Figs. 1B–C). The variants from Clade H contain six differences (E2G, K262R, L431I, A452T, M463V, and V465P); of these five are present in the engineered enzymes (Fig. 1D).

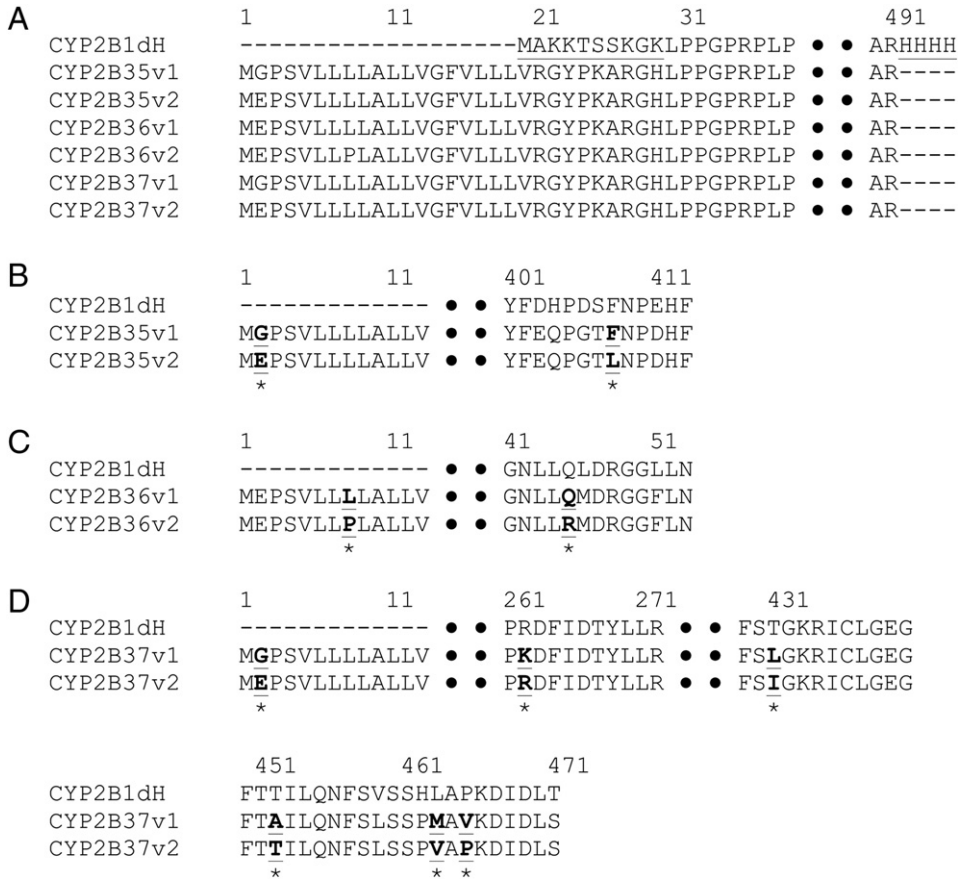

Fig. 1. Comparison of engineered rat 2B1 and full-length woodrat 2B35v1/2, 2B36v1/2, and 2B37v1/2. A) The *N*-terminal and *C*-terminal regions of engineered 2B1dH and the full-length woodrat enzymes. Amino acid numbering corresponds to the full-length position. Amino acid differences in the woodrat enzyme variants are shown underlined and bold for B) 2B35, C) 2B36, and D) 2B37. The *N*-terminal truncation and modification and *C*-terminal tetra-His tag found in 2B1dH were engineered into the woodrat 2B enzymes, so the first difference for each variant pair is not present in the engineered protein.

Amino acid differences present in the engineered enzymes are highlighted on homology models in Figs. 2A–C. Models were generated using the homology modeling program MODELLER (Eswar et al., 2008), the complete amino acid sequence of the engineered protein, and the CYP2B6-(+)-α-pinene complex (PDB: 4I91, (Wilderman et al., 2013)) with ligands and waters removed as the template. The heme is colored red in all panels. The amino acid sequences of the woodrat enzymes also show at least 87% identity to full-length rat 2B1.

Significant differences in expression levels were seen among engineered 2B35, 2B36, and 2B37 (Table 1). Each variant of 2B35 and 2B36 also showed different expression levels from its partner. 2B35v1 expressed in *Escherichia coli* at ~35% of the level of 2B1. 2B36v1 had expression levels about 20% higher than 2B1. For 2B35 and 2B36 variant one expressed at roughly 3.5-times the level of variant two. Both 2B37 variants expressed at similar levels to each other,~55–60% of the level of the engineered rat enzyme. Following engineering, 2B35v1, 2B36v1, and both variants of 2B37 were purified to homogeneity using a Ni^{2+}-NTA column followed by a Macroprep CM-Sepharose column. Characterization of 2B35v2 was not continued due to protein instability after elution from the Ni^{2+}-NTA column, and separation of 2B36v2 from RNA contamination during the purification process was not possible.

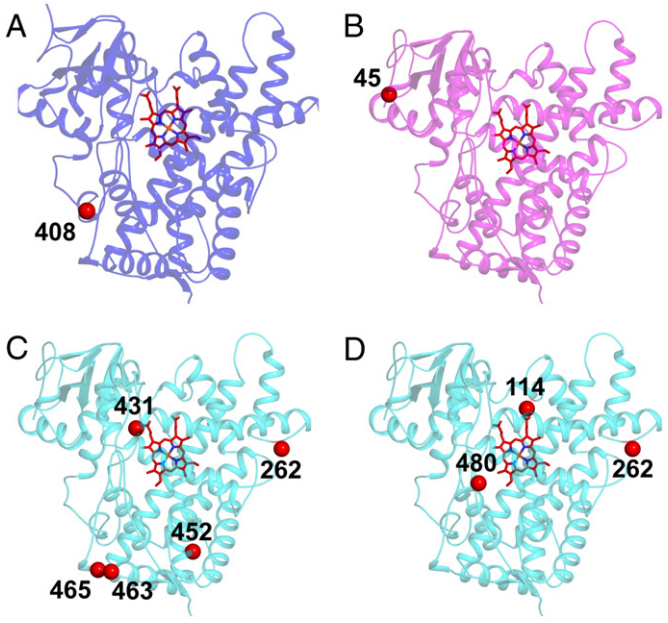

Fig. 2. Homology models showing the location of amino acid differences and mutants in woodrat 2B35, 2B36, and 2B37. A) 2B35v1 model in blue highlighting residue 408 in red. B) 2B36v1 model in magenta highlighting residue 45 in red. C) 2B37v2 model in cyan highlighting residues 262, 431, 452, 463, and 465 in red. D) 2B37v2 model showing the location of residues mutated for further analysis in this manuscript (114, 262, and 480).

7-EFC and 7-BR metabolism

Two model substrates for which CYP2B enzymes from other species have high selectivity are 7-ethoxy-4-trifluoromethylcoumarin (7-EFC) and 7-benzyloxyresorufin (7-BR). Steady-state kinetic measurements show unique profiles for each of the woodrat 2B enzymes (Table 1). With 2B35v1 *O*-dealkylation products were not detected for either

Table 1
Quantitative expression of, model substrate metabolism by, and (+)-α-pinene binding to rat 2B1 and wild-type woodrat 2B enzymes.

Protein (clade)	Quantitative expression[a] (nmol/L culture)	7-EFC O-deethylation[a]			7-BR O-debenzylation			(+)-α-Pinene spectral binding	
		k_{cat} (min^{-1})	K_M (μM)	k_{cat}/K_M (min^{-1} μM^{-1})	k_{cat} (min^{-1})	K_M (μM)	k_{cat}/K_M (min^{-1} μM^{-1})	K_S (μM)[a]	%HS_{P450}[b] Max Δ *Initial*
2B1	800 ± 50	6.9 ± 1.2	32.4 ± 4.9	0.21	4.6 ± 0.8	2.0 ± 0.6	2.3	0.87 ± 0.08	48.7 ± 1.3 *32.6 ± 1.5*
2B35v1 (A)	280 ± 30	ND[c]	–	–	ND[c]	–	–	1.27 ± 0.49	13.1 ± 1.6 *7.0 ± 0.3*
2B35v2 (A)[d]	55 ± 20	–	–	–	–	–	–	–	–
2B36v1 (F)	945 ± 80	3.3 ± 1.0	18.3 ± 7.0	0.18	0.10 ± 0.03	1.7 ± 0.3	0.06	0.58 ± 0.04	42.8 ± 7.2 *12.3 ± 1.0*
2B36v2 (F)[e]	270 ± 10	–	–	–	–	–	–	–	–
2B37v1 (H)	590 ± 30	10.0 ± 0.3	23.5 ± 2.0	0.43	0.16 ± 0.04	7.2 ± 0.6	0.02	9.33 ± 0.76	25.3 ± 0.5 *28.6 ± 1.7*
2B37v2 (H)	450 ± 30	14.5 ± 8.3	20.0 ± 4.2	0.73	0.25 ± 0.06	9.5 ± 0.5	0.03	0.91 ± 0.07	38.4 ± 0.7 *25.8 ± 1.4*

[a] Values are represented as the mean ± standard deviation of at least three independent experiments.
[b] HS_{P450}, high-spin P450.
[c] ND, not detected.
[d] 2B35v2 was not stable during the Ni^{2+}-NTA purification step.
[e] Separation of 2B36v2 from RNA during purification was not possible.

7-EFC or 7-BR. With 2B36v1 catalytic efficiency was similar to that of rat 2B1 for 7-EFC *O*-deethylation with k_{cat} about half that of 2B1 and K_M about two thirds that of 2B1. However the efficiency for 7-BR *O*-debenzylation by 2B36v1 was 1/40th that of 2B1. This result is almost entirely due to a much lower k_{cat}.

Using 7-EFC as a substrate, 2B37v1 displayed a k_{cat} that was ~1.4-fold higher than that for 2B1, and K_M was ~25% lower; the resulting catalytic efficiency for this substrate was ~1.8-fold higher than for 2B1. With 2B37v2, catalytic efficiency was ~2.5-fold greater than 2B1dH, which was almost entirely due to the higher k_{cat} compared with 2B1. Catalytic efficiency for metabolism of 7-BR by both variants of 2B37 was similar to that of 2B36v1. The decreased of the 2B37 variants compared with 2B1 is due to a combination of a markedly lower k_{cat} and a K_M roughly 3.5–4.5 times higher than the rat enzyme.

Spectral binding titrations

Spectral binding titrations were used to assess the interactions of a typical monoterpene that has been shown previously to be a potent inhibitor of CYP2B1 in rat liver microsomes. This class of compounds is found at high concentrations in juniper (Adams et al., 1981; De-Oliveira et al., 1997a, 1999). (+)-α-Pinene (Fig. 3A) induced a Type I difference spectra with a peak at ~388 nm and a trough at ~420 nm, as represented in Fig. 3B with 2B1. Plotting the change in the % HS_{P450} for each enzyme produced a curve similar to that displayed in Fig. 3C. Spectral binding affinities (K_S) for (+)-α-pinene were very similar among 2B1 and most of the woodrat enzymes (Table 1). The K_S for (+)-α-pinene was at least an order of magnitude weaker for 2B37v1 (~9 μM) than for the other enzymes. In addition to the high affinity of this ligand for CYP2B enzymes, the magnitude of the spin shift seen upon ligand binding is remarkable (Table 1). 2B1 showed the greatest maximum percent change in (HS_{P450}) content upon (+)-α-pinene binding, followed by 2B36v1, 2B37v2, 2B37v1, and 2B35v1.

Residue 262 in 2B37

In human 2B6, residue 262 is the location of a single nucleotide polymorphism (SNP). The replacement of lysine with arginine at this residue increases expression levels and protein solubility, and alters susceptibility to inhibition by various drugs (Talakad et al., 2009).

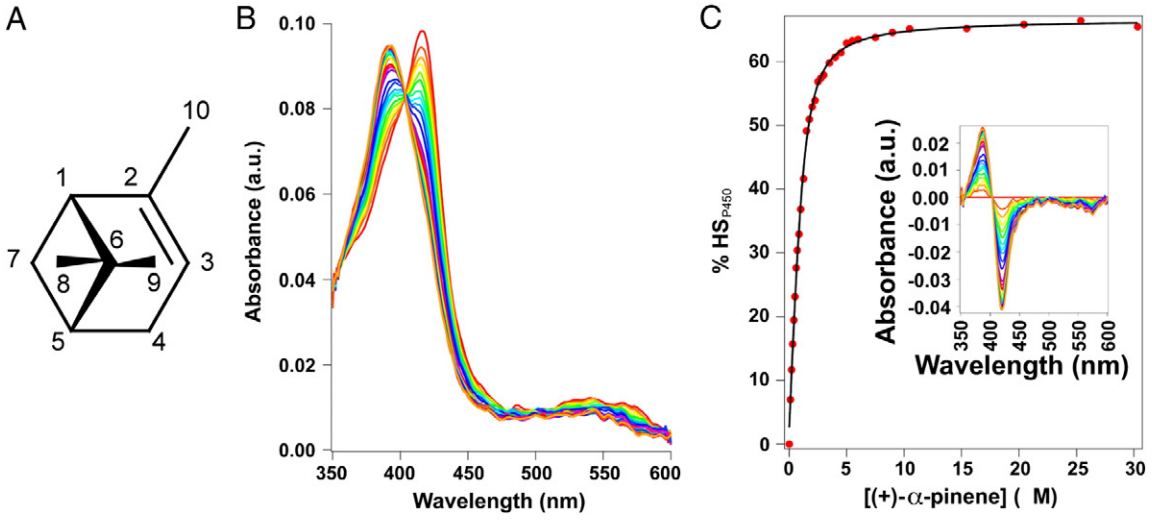

Fig. 3. CYP2B interaction with (+)-α-pinene. A) Chemical structure of (+)-α-pinene, a common monoterpene from plants, particularly juniper species. B) Absolute absorbance spectra from a titration of 2B1 with (+)-α-pinene. A distinct decrease in absorbance at 417 nm (low-spin state, LS_{P450}) and increase at 390 nm (high-spin state, HS_{P450}) is seen in these results. C) Plot of fraction HS_{P450} as a function of ligand concentration. Fitting to the ligand binding equation is shown.

Table 2
The effect of altering residue 262, a known site of genetic polymorphism in human 2B6, on clade H enzymes.

Protein	Quantitative expression[a] (nmol/L culture)	7-EFC O-deethylation[a]			7-BR O-debenzylation			(+)-α-Pinene spectral binding	
		k_{cat} (min^{-1})	K_M (μM)	k_{cat}/K_M (min^{-1} μM^{-1})	k_{cat} (min^{-1})	K_M (μM)	k_{cat}/K_M (min^{-1} μM^{-1})	K_S (μM)[a]	%HS_{P450}[b] Max Δ *Initial*
2B37v1	590 ± 30	10.0 ± 0.3	23.5 ± 2.0	0.43	0.16 ± 0.04	7.2 ± 0.6	0.02	9.33 ± 0.76	25.3 ± 0.5 *28.6 ± 1.7*
2B37v1 K262R	460 ± 40	5.4 ± 0.2	19.0 ± 2.3	0.28	0.15 ± 0.07	8.1 ± 0.7	0.02	2.04 ± 0.23	58.1 ± 1.2 *30.6 ± 0.9*
2B37v2	450 ± 30	14.5 ± 8.3	20.0 ± 4.2	0.73	0.25 ± 0.06	9.5 ± 0.5	0.03	0.91 ± 0.07	38.4 ± 0.7 *25.8 ± 1.4*
2B37v2 R262K	510 ± 60	2.0 ± 0.1	20.3 ± 2.8	0.10	0.18 ± 0.05	9.2 ± 0.7	0.02	1.06 ± 0.07	49.2 ± 0.4 *33.8 ± 1.3*

[a] Values are represented as the mean ± standard deviation of at least three independent experiments.
[b] HS_{P450}, high-spin P450.

Accordingly, the reciprocal mutants at position 262 (Fig. 2D) were made in the engineered 2B37v1 and 2B37v2. Effects on expression were small (Table 2). Introduction of arginine at residue 262 reduced the catalytic efficiency of 2B37v1 by ~35%, mainly due to a ~45% decrease in k_{cat}. Replacement of R262 with lysine in 2B37v2 had a much greater effect on oxidation of 7-EFC, yielding an 85% decrease in the catalytic efficiency. Much smaller decreases were seen in 7-BR *O*-dealkylation by these mutants, and virtually no change was seen in the catalytic efficiencies of this reaction. The K_S for (+)-α-pinene was four times lower for 2B37v1 K262R than for the wild-type enzyme, but the 2B37v2 R262K substitution had little effect on (+)-α-pinene K_S. The relative increase in high-spin hemoprotein content of wild-type 2B37v1 is ~90% with an initial content of 28.6% and an increase of 25.3%; this increase is ~145% for 2B37v2 (initial—25.8%, increase—38.4%). 2B37v1 K262R displays a relative increase of ~190% (initial—30.6%, increase—58.1%), and for 2B37v2 R262K the relative increase remains ~145% (initial—33.8%, increase—49.2%). Analysis of these changes using an independent sample *t*-test yielded *P*-values $\ll 0.001$.

Effects of altering residues 114 and 480

Residues 114 and 480 (Fig. 2D) play roles in substrate recognition and/or product profiles in various 2B enzymes (Zhao and Halpert, 2007). Dearing and coworkers noted that these residues and others in previously identified substrate recognition sites (SRS) show similarity within and variation across the phylogenetic clades identified from the sequence data (Malenke, et al., 2012). Thus, V114I, V480L, and V114I/V480L were created in 2B37v2 with the aim of engineering 2B36 metabolism profiles into 2B37. Each of these mutants showed less than 25% change in expression levels when compared with the wild-type enzyme (Table 3). These mutants displayed altered catalytic and binding activities from the wild-type 2B37v2, but none of these profiles were comparable to that of 2B36v1. With 7-EFC as a substrate the V114I mutant showed much lower catalytic efficiency than 2B37v2 due to a lower k_{cat} and much higher K_M, but V480L was roughly as efficient as the wild-type enzyme with a higher k_{cat} and lower K_M for 7-EFC. The double mutant V114I/V480L behaved in a manner more similar to the V480L mutant and wild-type 2B37v2 than the V114I mutant. Small changes in catalytic efficiency were seen with 7-BR with both single mutants. V114I had a lower k_{cat} and lower K_M for 7-BR than 2B37v2, and V480L had higher k_{cat} and lower K_M for this ligand. The double mutant, V114I/V480L, showed a low k_{cat}, but the K_M was greater than the solubility limit of the ligand in aqueous solutions (~10 μM) preventing determination of catalytic constants. The K_S of the mutants for (+)-α-pinene was lower than wild-type 2B37v2 by roughly a factor of three or more. These affinities were greater than that of 2B36v1. The effects on the K_S for (+)-α-pinene binding to each of the single mutants seem to be somewhat additive in the case of the double mutant. These mutations in 2B37v2 did not produce a pseudo-2B36v1, and each of the enzymes and mutants had a unique profile across the 7-EFC, 7-BR, and (+)-α-pinene assays.

Discussion

Despite the intense focus in recent years on the ligand recognition and binding step(s) in the CYP catalytic cycle, there is still uncertainty

Table 3
Changes at residues 114 and 480 alter enzyme activity in 2B37v2, but do not create a pseudo-clade F enzyme.

Protein (clade)	Quantitative expression[a] (nmol/L culture)	7-EFC O-deethylation[a]			7-BR O-debenzylation			(+)-α-Pinene spectral binding	
		k_{cat} (min^{-1})	K_M (μM)	k_{cat}/K_M (min^{-1} μM^{-1})	k_{cat} (min^{-1})	K_M (μM)	k_{cat}/K_M (min^{-1} μM^{-1})	K_S (μM)[a]	%HS_{P450}[b] Max Δ *Initial*
2B36v1 (F)	945 ± 80	3.3 ± 1.0	18.3 ± 7.0	0.18	0.10 ± 0.03	1.7 ± 0.3	0.06	0.58 ± 0.04	42.8 ± 7.2 *12.3 ± 1.0*
2B37v2 (H)	450 ± 30	14.5 ± 8.3	20.0 ± 4.2	0.73	0.25 ± 0.06	9.5 ± 0.5	0.03	0.91 ± 0.07	38.4 ± 0.7 *25.8 ± 1.4*
2B37v2 V114I	400 ± 30	6.3 ± 1.9	120 ± 2	0.05	0.13 ± 0.01	5.7 ± 1.0	0.02	0.36 ± 0.05	30.4 ± 3.5 *47.5 ± 1.8*
2B37v2 V480L	550 ± 70	22.3 ± 2.0	23.9 ± 3.6	0.93	0.47 ± 0.08	4.5 ± 0.7	0.10	0.18 ± 0.10	31.6 ± 1.5 *36.7 ± 1.2*
2B37v2 V114I/V480L	470 ± 50	20.8 ± 2.8	32.5 ± 4.4	0.64	ND[c]	>10[d]	ND[c]	0.25 ± 0.15	26.0 ± 3.5 *49.0 ± 2.1*

[a] Values are represented as the mean ± standard deviation of at least three independent experiments.
[b] HS_{P450}, high-spin P450.
[c] ND, not detected.
[d] 7-BR is not soluble in an aqueous solution at concentrations over~10 μM.

as to how a single enzyme handles a diverse assortment of xenobiotic compounds (Davydov and Halpert, 2008; Halpert, 2011; Isin and Guengerich, 2008; Wade et al., 2005). Data from a host of complementary techniques including NMR, molecular dynamics simulations, and X-ray crystallography indicate an integral role of protein dynamics in ligand binding and catalysis for many enzymes, including CYPs (Bakan and Bahar, 2009; Hays et al., 2004; Henzler-Wildman et al., 2007; Pochapsky et al., 2009; Savino et al., 2009). Furthermore, multiple recent studies of CYP2B enzymes focused on the role of both active site residues and non-active site residues in function and protein stability (Kumar et al., 2007; Talakad et al., 2010; Wilderman et al., 2012). The techniques used in such studies should be able to shed light on the selective process whereby wild herbivores adapt to changes in the plant secondary compound (PSC) profiles of their diets. However, systematic analysis of enzymes from wild mammalian herbivores has only recently begun (Malenke et al., 2012, 2013). The results presented here describe the characterization of CYP2B enzymes from individuals drawn from wild non-primate populations. Protein–ligand interactions were compared between rat 2B1 and the woodrat CYP2B enzymes. The results underscore the importance of small differences in amino acid sequences in the function of 2B enzymes. Furthermore, previously identified residues that determine protein–ligand interactions in rat, rabbit, human, and dog CYP2B enzymes, including residues 114, 262, and 480, fail to account for functional differences among the various woodrat enzymes.

Characterization of the woodrat CYP2B enzymes was initiated by examination of steady-state kinetics of the oxidation of the model CYP2B substrates 7-EFC and 7-BR. Both variants of 2B37 were studied, whereas 2B35v2 and 2B36v2 could not be purified with our standard chromatographic procedure. Of the purified enzymes, 2B35v1 did not show dealkylation activity in either assay. 2B36v1 turned over 7-EFC about as efficiently as 2B1, but had a much lower k_{cat} for 7-BR *O*-debenzylation than 2B1 (~0.10 vs. ~4.5). In comparison to rat 2B1, the 2B37 variants had similar K_M values for 7-EFC. The k_{cat} for 7-EFC-*O*-deethylation by 2B37v1 and 2B37v2 was ~50% and 2-fold greater than that of 2B1, respectively. Similar to 2B36v1, the 2B37 variants were much less efficient at catalyzing *O*-debenzylation of 7-BR than 2B1. The lower catalytic efficiency in the 7-BR assay with 2B36v1 and the 2B37 variants does not rule out more efficient dealkylation of other resorufin derivatives by these enzymes. Similarly, 2B35v1 might show activity with other coumarin or resorufin derivatives. Furthermore, the possibility of oxidation events other than 7-dealkylation occurring is not excluded, as was seen in mutants of 2B1 and human 3A4 probed using 7-alkoxycoumarins of varying chain length (Khan and Halpert, 2000; Kobayashi et al., 1998).

In addition to catalytic studies, CYP2B interactions with a natural product encountered in a wild diet were examined. The ligand probe used here, (+)-α-pinene, is a monoterpene that occurs in the diets of woodrats (Mabry et al., 1977) and is also a component of the diets and the environments of other herbivorous and omnivorous species (rabbit, rat, human). CYP2B enzymes had previously been linked to interactions with a range of monoterpenoids including (+)-α-pinene (Fig. 2A) (De-Oliveira et al., 1997a, 1999; Miyazawa and Gyoubu, 2007; Miyazawa et al., 2003; Wilderman et al., 2013). Interestingly, (+)-α-pinene is a pure hydrocarbon and produces a marked increase in HS_{P450} content when each of the enzymes is saturated with the ligand (Table 3, Figs. 2B–C). For reference, the drugs clopidogrel, sertraline, and ticlopidine bind with low micromolar K_S values and induce maximal increases in HS_{P450} content upon binding to human 2B6 of only 2.6%, 0.8%, and 2.3%, respectively (Talakad et al., 2009). Even the relatively lower spin shift upon (+)-α-pinene binding to 2B35v1, is more than 5-times higher than that of clopidogrel with 2B6. (+)-α-Pinene binds with very high affinity to 2B1 and three of the woodrat enzymes tested, 2B35v1, 2B36v1, and 2B37v2 but shows significantly lower binding affinity for 2B37v1 (Table 3). Since only five residues in the engineered 2B37v1 and 2B37v2 are different, one or more of these amino acid differences should explain these large differences in spectral binding affinity between the two enzymes.

While (+)-α-pinene has been linked to CYP2B enzymes, terpenoids in general have been linked to multiple CYP enzymes. In addition to CYP2B enzymes from rat, rabbit, and human, (+)-α-pinene is also metabolized by CYP101A1 ($P450_{cam}$) (Bell et al., 2002). A mixture of terpenoids, including 1,8-cineole and (+)-α-pinene, induced expression of CYP enzymes that reacted with antibodies to human CYP2E1 and rat CYP2C6 and CYP2C11 in experiments with common brushtail possoms (Pass et al., 1999). However, 1,8-cineole was primarily turned over by CYP3A4 in experiments using human liver microsomes and recombinant CYP enzymes (Duisken et al., 2005). The monoterpene β-myrcene induces expression of CYP2B enzymes in rat, and multiple monoterpenoids inhibit CYP2B1 function in rat liver microsomes (De-Oliveira et al., 1997a,b). Furthermore, CYP2B enzymes oxidize (−)-α-pinene in rabbit and human (Noma and Asakawa, 2009). Limonene is metabolized by CYP2C11 in untreated rats and by CYP2B1 in phenobarbital treated rats but by CYP2C9 and CYP2C19 in humans (Miyazawa et al., 2001, 2002). The ketones (−)-fenchone and (−)-verbenone are metabolized by CYP2A6 and 2B6 in humans, but (−)-verbenone is metabolized by CYP2C11 and CYP2B1 in rats (Miyazawa and Gyoubu, 2007; Miyazawa et al., 2003). Based on this evidence, herbivore response to monoterpenoid challenge is likely species specific, and while the possibility exists that another CYP enzyme might be the primary route of processing (+)-α-pinene in *Neotoma* species, the chemical properties of the molecule match the general description of a CYP2B substrate in terms of lipophilicity (log P = 4.44), molecular shape, and relative molecular mass (M_r = 136.23) (Sridhar et al., 2012).

The topic of residues important for governing substrate specificity, product production, and individual variability in humans has been well studied in CYP2B enzymes (Domanski and Halpert, 2001; Ingelman-Sundberg, 2004; Mo et al., 2009; Zanger and Schwab, 2013; Zhao and Halpert, 2007). In 2B37, mutation of residue 262 had small effects on K_M for the substrate 7-EFC, but large changes were seen in k_{cat} and catalytic efficiency. Two expected results of reduced k_{cat} are a lower rate of clearance of potential toxins and a diminished ability to deal with increases in the dietary levels of PSCs. Interestingly, mutation of this residue in 2B6 causes little difference in k_{cat} for 7-MFC oxidation, but there are significant differences in protein–ligand interactions, specifically competitive inhibition, for multiple important drugs including ticlopidine (Talakad et al., 2009). Mutation of residues 114 and/or 480 in identified substrate recognition sequences did not change the function of 2B37v2 to that of 2B36v1. In rat 2B1 residue 114 is a major determinant of substrate specificity, and the importance of residue 480 was shown in dog 2B11 (Hasler et al., 1994; Liu et al., 1996). Since residues previously implicated in substrate recognition did not markedly alter the preferences of 2B37v2, other amino acid differences yet to be identified and investigated between 2B36v1 and 2B37v2 must govern the differences in ligand recognition.

The functional differences among 2B35, 2B36, and 2B37 are of interest in the context of geographically distinct woodrat populations. Animals from the Mojave Desert regularly consume large amounts of creosote bush (*L. tridentata*), which contains resin dominated by phenolic compounds, while the diet of animals from the Great Basin population has a high percentage of juniper foliage, a plant rich in terpenes. Juniper is not currently found in the Mojave but is thought to be a part of the ancient flora displaced as a result of the natural climate change that occurred ~18,000 years ago (Hunter et al., 2001). Malenke and coworkers noticed that 2B35 was present in both woodrat populations, but the other enzymes were predominantly isolated from either the Great Basin (2B36) or the Mojave Desert (2B37) (Malenke et al., 2012). Based on this information we propose that 2B35 may be a general detoxification mechanism for woodrats, and 2B36 and 2B37 have evolved to deal with the unique PSC profiles from their diets. Future work characterizing the function of these and other woodrat CYP2B enzymes may reveal additional novel functions related to specific endogenous compounds, PSCs, or to the wide breadth of compounds encountered by these generalist herbivores in their daily diet.

The genus *Neotoma* has been used as an experimental system to study plant–herbivore interactions because its members have disparate plant diets that differ across species and habitats. Most *Neotoma* species consume plants with high levels of secondary compounds, which present a considerable toxic challenge to these herbivores. In response, woodrats have evolved a variety of mechanisms for dealing with these toxins including caching behaviors, efflux transporters in the gut, bacterial endosymbioses, and liver enzyme biotransformation (Haley et al., 2008; Kohl and Dearing, 2012; Sorensen and Dearing, 2003; Torregrossa and Dearing, 2009). The importance of the liver in biotransformation has been demonstrated multiple times within *Neotoma*, but the question remains as to how liver enzymes have adapted to the challenges of ingesting diets containing complex mixtures of potential toxins (Haley et al., 2007b, 2008). The comparative data presented here on woodrat CYP2B enzymes begin to answer this question by showing further evidence that small changes in protein sequence have large effects on metabolism of substrates and that ecologically relevant biochemical assays (such as the monoterpene binding assay) may reveal hitherto unknown function.

Conflict of interest statement

The authors declare no conflicts of interest.

Acknowledgments

This research was supported by the National Institutes of Health (grant number ES003619 to J.R.H.) and the National Science Foundation grants IOS 1256840 to J.R.H. and 0817527 to M.D.D. P.R.W. was supported in part by the Training Grant in Heme and Blood Proteins from the National Institutes of Health (grant number T32-DK07233).

Appendix A. Supplementary data

Supplementary data to this article can be found online at http://dx.doi.org/10.1016/j.taap.2013.12.005.

References

Adams, R.P., Zanoni, T.A., Vonrudloff, E., Hogge, L., 1981. The southwestern USA and northern Mexico one-seeded junipers—their volatile oils and evolution. Biochem. Syst. Ecol. 9, 93–96.
Al Omari, A., Murry, D.J., 2007. Pharmacogenetics of the cytochrome P450 enzyme system: review of current knowledge and clinical significance. J. Pharm. Pract. 20, 206–218.
Anzenbacher, P., Anzenbacherova, E., Lange, R., Skopalik, J., Otyepka, M., 2008. Active sites of cytochromes P450: what are they like? Acta Chim. Slov. 55, 63–66.
Bakan, A., Bahar, I., 2009. The intrinsic dynamics of enzymes plays a dominant role in determining the structural changes induced upon inhibitor binding. Proc. Natl. Acad. Sci. U. S. A. 106, 14349–14354.
Bell, S.G., Chen, X., Sowden, R.J., Xu, F., Williams, J.N., Wong, L.-L., Rao, Z., 2002. Molecular recognition in (+)-α-pinene oxidation by cytochrome P450cam. J. Am. Chem. Soc. 125, 705–714.
Davydov, D.R., Halpert, J.R., 2008. Allosteric P450 mechanisms: multiple binding sites, multiple conformers or both? Expert Opin. Drug Metab. Toxicol. 4, 1523–1535.
Davydov, D.R., Deprez, E., Hui Bon Hoa, G., Knyushko, T.V., Kuznetsova, G.P., Koen, Y.M., Archakov, A.I., 1995. High-pressure-induced transitions in microsomal cytochrome P450 2B4 in solution: evidence for conformational inhomogeneity in the oligomers. Arch. Biochem. Biophys. 320, 330–344.
Dearing, M.D., Foley, W.J., McLean, S., 2005. The influence of plant secondary metabolites on the nutritional ecology of herbivorous terrestrial vertebrates. Annu. Rev. Ecol. Evol. Syst. 36, 169–189.
DeLano, W., 2009. The PyMOL Molecular Graphics System MacPyMOL.
De-Oliveira, A., RibeiroPinto, L.F., Paumgartten, F.J.R., 1997a. In vitro inhibition of CYP2B1 monooxygenase by β-myrcene and other monoterpenoid compounds. Toxicol. Lett. 92, 39–46.
De-Oliveira, A.C., Ribeiro-Pinto, L.F., Otto, S.S., Goncalves, A., Paumgartten, F.J., 1997b. Induction of liver monooxygenases by beta-myrcene. Toxicology 124, 135–140.
De-Oliveira, A., Fidalgo-Neto, A.A., Paumgartten, F.J.R., 1999. In vitro inhibition of liver monooxygenases by β-ionone, 1,8-cineole, (−)-menthol and terpineol. Toxicology 135, 33–41.
Domanski, T.L., Halpert, J.R., 2001. Analysis of mammalian cytochrome P450 structure and function by site-directed mutagenesis. Curr. Drug Metab. 2, 117–137.
Duisken, M., Sandner, F., Blömeke, B., Hollender, J., 2005. Metabolism of 1,8-cineole by human cytochrome P450 enzymes: identification of a new hydroxylated metabolite. Biochim. Biophys. Acta Gen. Subj. 1722, 304–311.
El-Merhibi, A., Ngo, S., Jones, B., Milic, N., Stupans, I., Mckinnon, R., 2008. Molecular insights into xenobiotic disposition in Australian marsupials. Australas. J. Ecotoxicol. 13, 53–64.
El-Merhibi, A., Ngo, S.N.T., Crittenden, T.A., Marchant, C.L., Stupans, I., McKinnon, R.A., 2011. Cytochrome P450 CYP3A in marsupials: cloning and characterisation of the second identified CYP3A subfamily member, isoform 3A78 from koala (*Phascolarctos cinereus*). Comp. Biochem. Physiol. C 154, 367–376.
El-Merhibi, A., Ngo, S.N.T., Marchant, C.L., Height, T.A., Stupans, I., McKinnon, R.A., 2012. Cytochrome P450 CYP3A in marsupials: cloning and identification of the first CYP3A subfamily member, isoform 3A70 from Eastern gray kangaroo (*Macropus giganteus*). Gene 506, 423–428.
Eswar, N., Eramian, D., Webb, B., Shen, M.Y., Sali, A., 2008. Protein structure modeling with MODELLER. Methods Mol. Biol. 426, 145–159.
Gay, S.C., Roberts, A.G., Halpert, J.R., 2010. Structural features of cytochromes P450 and ligands that affect drug metabolism as revealed by X-ray crystallography and NMR. Futur. Med. Chem. 2, 1451–1468.
Gonzalez, F.J., 1988. The molecular-biology of cytochrome P450s. Pharmacol. Rev. 40, 243–288.
Guengerich, F.P., 2001. Common and uncommon cytochrome P450 reactions related to metabolism and chemical toxicity. Chem. Res. Toxicol. 14, 611–650.
Guengerich, F.P., Isin, E.M., 2008. Mechanisms of cytochrome P450 reactions. Acta Chim. Slov. 55, 7–19.
Haley, S.L., Lamb, J.G., Franklin, M.R., Constance, J.E., Dearing, M.D., 2007a. Xenobiotic metabolism of plant secondary compounds in juniper (*Juniperus monosperma*) by specialist and generalist woodrat herbivores, genus *Neotoma*. Comp. Biochem. Physiol. C 146, 552–560.
Haley, S.L., Lamb, J.G., Franklin, M.R., Constance, J.E., Dearing, M.D., 2007b. Xenobiotic metabolism of plant secondary compounds in oak (*Quercus agrifolia*) by specialist and generalist woodrat herbivores, genus *Neotoma*. J. Chem. Ecol. 33, 2111–2122.
Haley, S.L., Lamb, J.G., Franklin, M.R., Constance, J.E., Dearing, M.D., 2008. "Pharm-Ecology" of diet shifting: biotransformation of plant secondary compounds in creosote (*Larrea tridentata*) by a woodrat herbivore, *Neotoma lepida*. Physiol. Biochem. Zool. 81, 584–593.
Halpert, J.R., 2011. Structure and function of cytochromes P450 2B: from mechanism-based inactivators to X-ray crystal structures and back. Drug Metab. Dispos. 39, 1113–1121.
Harlow, G.R., Halpert, J.R., 1997. Alanine-scanning mutagenesis of a putative substrate recognition site in human cytochrome P450 3A4. Role of residues 210 and 211 in flavonoid activation and substrate specificity. J. Biol. Chem. 272, 5396–5402.
Hasler, J.A., Harlow, G.R., Szklarz, G.D., John, G.H., Kedzie, K.M., Burnett, V.L., He, Y.A., Kaminsky, L.S., Halpert, J.R., 1994. Site-directed mutagenesis of putative substrate recognition sites in cytochrome P450 2B11: importance of amino acid residues 114, 290, and 363 for substrate specificity. Mol. Pharmacol. 46, 338–345.
Hays, A.M.A., Dunn, A.R., Chiu, R., Gray, H.B., Stout, C.D., Goodin, D.B., 2004. Conformational states of cytochrome P450cam revealed by trapping of synthetic molecular wires. J. Mol. Biol. 344, 455–469.
He, Y.Q., He, Y.A., Halpert, J.R., 1995. *Escherichia coli* expression of site-directed mutants of cytochrome-P450 2B1 from 6 substrate recognition sites—substrate-specificity and inhibitor selectivity studies. Chem. Res. Toxicol. 8, 574–579.
Henzler-Wildman, K.A., Lei, M., Thai, V., Kerns, S.J., Karplus, M., Kern, D., 2007. A hierarchy of timescales in protein dynamics is linked to enzyme catalysis. Nature 450, 913–916.
Holmans, P.L., Shet, M.S., Martin-Wixtrom, C.A., Fisher, C.W., Estabrook, R.W., 1994. The high-level expression in *Escherichia coli* of the membrane-bound form of human and rat cytochrome b5 and studies on their mechanism of function. Arch. Biochem. Biophys. 312, 554–565.
Hunter, K.L., Betancourt, J.L., Riddle, B.R., Van Devender, T.R., Cole, K.L., Spaulding, W.G., 2001. Ploidy race distributions since the last glacial maximum in the North American desert shrub, *Larrea tridentata*. Global Ecol. Biogeogr. 10, 521–533.
Ingelman-Sundberg, M., 2004. Human drug metabolising cytochrome P450 enzymes: properties and polymorphisms. Naunyn Schmiedeberg's Arch. Pharmacol. 369, 89–104.
Isin, E., Guengerich, F., 2008. Substrate binding to cytochromes P450. Anal. Bioanal. Chem. 392, 1019–1030.
Johnson, E.F., Stout, C.D., 2013. Structural diversity of eukaryotic membrane cytochrome P450s. J. Biol. Chem. 288, 17082–17090.
Khan, K.K., Halpert, J.R., 2000. Structure–function analysis of human cytochrome P450 3A4 using 7-alkoxycoumarins as active-site probes. Arch. Biochem. Biophys. 373, 335–345.
Kobayashi, Y., Fang, X., Szklarz, G.D., Halpert, J.R., 1998. Probing the active site of cytochrome P450 2B1: metabolism of 7-alkoxycoumarins by the wild type and five site-directed mutants. Biochemistry 37, 6679–6688.
Kohl, K.D., Dearing, M.D., 2012. Experience matters: prior exposure to plant toxins enhances diversity of gut microbes in herbivores. Ecol. Lett. 15, 1008–1015.
Kumar, S., Chen, C.S., Waxman, D.J., Halpert, J.R., 2005. Directed evolution of mammalian cytochrome P450 2B1: mutations outside of the active site enhance the metabolism of several substrates, including the anticancer prodrugs cyclophosphamide and ifosfamide. J. Biol. Chem. 280, 19569–19575.
Kumar, S., Zhao, Y., Sun, L., Negi, S.S., Halpert, J.R., Muralidhara, B.K., 2007. Rational engineering of human cytochrome P450 2B6 for enhanced expression and stability: importance of a Leu264->Phe substitution. Mol. Pharmacol. 72, 1191–1199.
Liu, J., He, Y.A., Halpert, J.R., 1996. Role of residue 480 in substrate specificity of cytochrome P450 2B5 and 2B11. Arch. Biochem. Biophys. 327, 167–173.
Mabry, T., Difeo, D., Sakakibara, M., Bohnstedt, C., Seigler, D., 1977. The natural products chemistry of Larrea. In: Mabry, T., Hunzike, J., Difeo, D. (Eds.), Creosote Bush: Biology

and Chemistry of Larrea in New World Deserts. Academic Press, New York, pp. 115–134.
Magnanou, E., Malenke, J.R., Dearing, M.D., 2009. Expression of biotransformation genes in woodrat (*Neotoma*) herbivores on novel and ancestral diets: identification of candidate genes responsible for dietary shifts. Mol. Ecol. 18, 2401–2414.
Malenke, J.R., Magnanou, E., Thomas, K., Dearing, M.D., 2012. Cytochrome P450 2B diversity and dietary novelty in the herbivorous, desert woodrat (*Neotoma lepida*). PLoS One 7, e41510.
Malenke, J.R., Milash, B., Miller, A.W., Dearing, M.D., 2013. Transcriptome sequencing and microarray development for the woodrat (*Neotoma* spp.): custom genetic tools for exploring herbivore ecology. Mol. Ecol. Resour. 13, 674–687.
Mangione, A.M., Dearing, M.D., Karasov, W.H., 2000. Interpopulation differences in tolerance to creosote bush resin in desert woodrats (*Neotoma lepida*). Ecology 81, 2067–2076.
Miyazawa, M., Gyoubu, K., 2007. Metabolism of (−)-fenchone by CYP2A6 and CYP2B6 in human liver microsomes. Xenobiotica 37, 194–204.
Miyazawa, M., Shindo, M., Shimada, T., 2001. Sex differences in the metabolism of (+)- and (−)-limonene enantiomers to carveol and perillyl alcohol derivatives by cytochrome P450 enzymes in rat liver microsomes. Chem. Res. Toxicol. 15, 15–20.
Miyazawa, M., Shindo, M., Shimada, T., 2002. Metabolism of (+)- and (−)-limonenes to respective carveols and perillyl alcohols by CYP2C9 and CYP2C19 in human liver microsomes. Drug Metab. Dispos. 30, 602–607.
Miyazawa, M., Sugie, A., Shimada, T., 2003. Roles of human CYP2A6 and 2B6 and rat CYP2C11 and 2B1 in the 10-hydroxylation of (−)-verbenone by liver microsomes. Drug Metab. Dispos. 31, 1049–1053.
Mo, S.L., Liu, Y.H., Duan, W., Wei, M.Q., Kanwar, J.R., Zhou, S.F., 2009. Substrate specificity, regulation, and polymorphism of human cytochrome P450 2B6. Curr. Drug Metab. 10, 730–753.
Muralidhara, B.K., Negi, S., Chin, C.C., Braun, W., Halpert, J.R., 2006. Conformational flexibility of mammalian cytochrome P450 2B4 in binding imidazole inhibitors with different ring chemistry and side chains: solution thermodynamics and molecular modeling. J. Biol. Chem. 281, 8051–8061.
Ngo, S.N.T., McKinnon, R.A., Stupans, I., 2003. The effects of *Eucalyptus* terpenes on hepatic cytochrome P450 CYP4A, peroxisomal Acyl CoA oxidase (AOX) and peroxisome proliferator activated receptor alpha (PPARα) in the common brush tail possum (*Trichosurus vulpecula*). Comp. Biochem. Physiol. C 136, 165–173.
Ngo, S.N.T., McKinnon, R.A., Stupans, I., 2006. Cloning and expression of koala (*Phascolarctos cinereus*) liver cytochrome P450CYP4A15. Gene 376, 123–132.
Noma, Y., Asakawa, Y., 2009. Biotransformation of monoterpenoids by microorganisms, insects, and mammals. In: Baser, K.H.C., Buchbauer, G. (Eds.), Handbook of Essential Oils: Science, Technology, and Applications. CRC Press, Boca Raton, pp. 585–736.
Omura, T., Sato, R., 1964. Carbon monoxide-binding pigment of liver microsomes. I. Evidence for its hemoprotein nature. J. Biol. Chem. 239, 2370–2378.
Omura, T., Sato, R., Cooper, D.Y., Rosenthal, O., Estabrook, R.W., 1965. Function of cytochrome P-450 of microsomes. Fed. Proc. 24, 1181–1189.
Otyepka, M., Berka, K., Anzenbacher, P., 2012. Is there a relationship between the substrate preferences and structural flexibility of cytochromes P450? Curr. Drug Metab. 13, 130–142.
Pass, G.J., McLean, S., Stupans, I., 1999. Induction of xenobiotic metabolising enzymes in the common brushtail possum, *Trichosurus vulpecula*, by *Eucalyptus* terpenes. Comp. Biochem. Physiol. C 124, 239–246.
Pochapsky, S.S., Dang, M., OuYang, B., Simorellis, A.K., Pochapsky, T.C., 2009. Redox-dependent dynamics in cytochrome P450cam. Biochemistry 48, 4254–4261.
Poulos, T.L., 2005a. Structural and functional diversity in heme monooxygenases. Drug Metab. Dispos. 33, 10–18.
Poulos, T.L., 2005b. Structural biology of heme monooxygenases. Biochem. Biophys. Res. Commun. 338, 337–345.
Savino, C., Montemiglio, L.C., Sciara, G., Miele, A.E., Kendrew, S.G., Jemth, P., Gianni, S., Vallone, B., 2009. Investigating the structural plasticity of a cytochrome P450: Three-dimensional structures of P450 eryK and binding to its physiological substrate. J. Biol. Chem. 284, 29170–29179.
Scott, E.E., Spatzenegger, M., Halpert, J.R., 2001. A truncation of 2B subfamily cytochromes P450 yields increased expression levels, increased solubility, and decreased aggregation while retaining function. Arch. Biochem. Biophys. 395, 57–68.
Shah, M.B., Wilderman, P.R., Pascual, J., Zhang, Q., Stout, C.D., Halpert, J.R., 2012. Conformational adaptation of human cytochrome P450 2B6 and rabbit cytochrome P450 2B4 revealed upon binding multiple amlodipine molecules. Biochemistry 51, 7225–7238.
Skopec, M.M., Haley, S., Dearing, M.D., 2007. Differential hepatic gene expression of a dietary specialist (*Neotoma stephensi*) and generalist (*Neotoma albigula*) in response to juniper (*Juniperus monosperma*) ingestion. Comp. Biochem. Physiol. D 2, 34–43.
Sorensen, J.S., Dearing, M.D., 2003. Elimination of plant toxins by herbivorous woodrats: revisiting an explanation for dietary specialization in mammalian herbivores. Oecologia 134, 88–94.
Sridhar, J., Liu, J.W., Foroozesh, M., Stevens, C.L.K., 2012. Insights on cytochrome P450 enzymes and inhibitors obtained through QSAR studies. Molecules 17, 9283–9305.
Stamp, N., 2003. Out of the quagmire of plant defense hypotheses. Q. Rev. Biol. 78, 23–55.
Talakad, J.C., Kumar, S., Halpert, J.R., 2009. Decreased susceptibility of the cytochrome P450 2B6 variant K262R to inhibition by several clinically important drugs. Drug Metab. Dispos. 37, 644–650.
Talakad, J.C., Wilderman, P.R., Davydov, D.R., Kumar, S., Halpert, J.R., 2010. Rational engineering of cytochromes P450 2B6 and 2B11 for enhanced stability: insights into structural importance of residue 334. Arch. Biochem. Biophys. 494, 151–158.
Torregrossa, A.M., Dearing, M.D., 2009. Caching as a behavioral mechanism to reduce toxin intake. J. Mammal. 90, 803–810.
Wade, R.C., Motiejunas, D., Schleinkofer, K., Sudarko, Winn, P.J., Banerjee, A., Kaniakin, A., Jung, C., 2005. Multiple molecular recognition mechanisms. Cytochrome P450—a case study. Biochim. Biophys. Acta Protein Proteomics 1754, 239–244.
Weng, J.-K., Philippe, R.N., Noel, J.P., 2012. The rise of chemodiversity in plants. Science 336, 1667–1670.
Wilderman, P.R., Halpert, J.R., 2012. Plasticity of CYP2B enzymes: structural and solution biophysical methods. Curr. Drug Metab. 13, 167–176.
Wilderman, P.R., Gay, S.C., Jang, H.H., Zhang, Q., Stout, C.D., Halpert, J.R., 2012. Investigation by site-directed mutagenesis of the role of cytochrome P450 2B4 non-active-site residues in protein–ligand interactions based on crystal structures of the ligand-bound enzyme. FEBS J. 279, 1607–1620.
Wilderman, P.R., Shah, M.B., Jang, H.H., Stout, C.D., Halpert, J.R., 2013. Structural and thermodynamic basis of (+)-α-pinene binding to human cytochrome P450 2B6. J. Am. Chem. Soc. 135, 10433–10440.
Zanger, U.M., Schwab, M., 2013. Cytochrome P450 enzymes in drug metabolism: regulation of gene expression, enzyme activities, and impact of genetic variation. Pharmacol. Ther. 138, 103–141.
Zhao, Y., Halpert, J.R., 2007. Structure–function analysis of cytochromes P450 2B. Biochim. Biophys. Acta Gen. Subj. 1770, 402–412.